

# Gas-Enrichment at Liquid-Wall Interfaces

Stephan M. Dammer and Detlef Lohse

*Department of Applied Physics, University of Twente, 7500 AE Enschede, The Netherlands*

(Dated: November 24, 2018)

Molecular dynamics simulations are performed to study the effects of dissolved gas on liquid-wall and liquid-gas interfaces. The systems are composed of different particle species (liquid/gas/wall) that interact via Lennard-Jones potentials. Liquid-gas mixtures in contact with walls exhibit gas enrichment at the walls, which increases with increasing hydrophobicity, quantified by the contact angle which is obtained from additional simulations of droplets at walls. When compared to the gas concentration in the bulk of the liquid, for hydrophobic walls the observed gas enrichment can exceed more than two orders of magnitude, which will favor bubble nucleation and slippage. Close to the walls the liquid shows a layered structure which is less pronounced for increasing contact angle and which for large contact angle is considerably altered by the presence of a gas. Also at liquid-gas interfaces gas enrichment is found which reduces the surface tension.

PACS numbers: 68.08.-p,68.03.-g,68.15.+e,83.50.Rp

The precise determination of the hydrodynamic boundary condition, *slip* vs. *no-slip*, is currently a matter of active debate. There is a growing number of studies, experiments [1, 2, 3, 4] as well as simulations [5, 6, 7] (and references therein), which strongly suggest that the classical no-slip condition, a more than 200 year old dogma, is violated. Though it is difficult to identify clear trends, the investigations suggest that increasing hydrophobicity and an increasing amount of dissolved gas in the liquid favor larger slip. Note, however, that slip has been reported for hydrophilic surfaces as well [4].

What is the cause of wall slippage? Despite many investigations, slippage behavior and its origin are far from being understood. A possible cause [1, 8] is the presence of so-called *surface nanobubbles*, i.e., nanoscale bubbles located on a solid surface that is immersed in liquid. It is evident that, if nanobubbles do indeed cover a sizeable fraction of the solid, this would result in a reduced adhesion force which would explain the observation of slip. Moreover, there are many recent experiments that strongly support the notion of surface nanobubbles, in particular atomic force microscopy measurements [9, 10, 11], but also other techniques [12, 13]. Similar to the trends for wall slip, hydrophobicity and dissolved gas favor surface nanobubbles. These are found on hydrophobic surfaces *and* gas-saturated liquid, whereas usually nanobubbles are not observed for hydrophilic *and/or* degassed liquid, suggesting gas- rather than vapor bubbles. In spite of growing experimental evidence for their existence, it is unclear how and why they form and why they are apparently stable.

Molecular dynamics simulations are a promising approach to investigate these questions. However, previous simulations of nanoscale bubbles [14] or slippage [5, 6, 7] were restricted to pure liquids instead of liquid-gas mixtures, although there is, as mentioned above, strong experimental evidence for the importance of dissolved gas. How do gases effect liquid-wall interfaces? How do the ef-

fects change with varying hydrophobicity? It is the aim of this Letter to address these issues by means of molecular dynamics simulations. Control parameters are the *dissolved gas concentration*, which has not been focused on before, and the *hydrophobicity of the wall*, which is quantified by numerical contact angle measurements. Liquid-gas interfaces which serve as reference systems and are important in their own right [15] are studied as well.

Simulations are performed for fixed particle number, volume and temperature  $T = 300$  K using the GROMACS code [16]. Periodic boundary conditions (p.b.c.) are applied in  $x$ ,  $y$ - and  $z$ -direction. Three different particle species (liquid/gas/wall) are simulated, all having the same molecular diameter  $\sigma = 0.34$  nm and the same mass  $m = 20$  amu. Particles interact via Lennard-Jones 6-12 potentials with a cutoff  $r_c = 5\sigma$ . Note that this cutoff is larger than the value  $2.5\sigma$  usually applied for bulk liquids, in order to account for inhomogeneities at interfaces. The energy scale  $\epsilon_{ll}$  for liquid-liquid interactions is fixed to  $\epsilon_{ll} \approx 1.2k_B T$  with Boltzmann's constant  $k_B$ . To model an inert gas, the energy scales for the gas interactions are fixed to  $\epsilon_{gg} = \epsilon_{gl} = \epsilon_{gw} \approx 0.4k_B T$ . The values of  $\sigma$  and  $\epsilon_{gg}$  are close to those of Argon. The temperature is below (above) the critical temperature of the liquid (gas) particles. The time step is  $dt = 0.005\tau$  with the characteristic time  $\tau = \sigma\sqrt{m/\epsilon_{ll}} \approx 0.9$  ps. During production runs, the simulations are weakly coupled to a heat bath using the Berendsen thermostat [17] with a relaxation time  $\tau_T = 10\tau$ . A perfectly stiff wall is simulated by solid particles that are frozen on a fcc-lattice with density  $\rho_w \approx 0.96\sigma^{-3}$ . Two *microscopic control parameters* are tuned which change the properties of interest: (i) the number of gas particles  $N_g$  and (ii) the ratio  $\epsilon_{lw}/\epsilon_{ll}$  with the scale  $\epsilon_{lw}$  for liquid-wall interactions. These microscopic parameters determine *macroscopic* properties such as the gas concentration and the contact angle.

Before addressing liquid-gas mixtures at walls it is worth discussing liquid-gas mixtures without walls as a

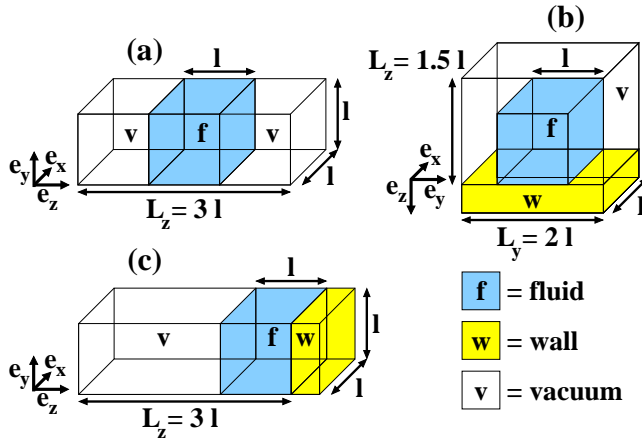


FIG. 1: (color) Starting configurations to study (a) liquid-gas interfaces, (b) droplets and (c) fluid films. Initially the 'fluid cube' is composed of particles on a lattice, which 'melts' during equilibration, forming a liquid while the vacuum is filled by a vapor-gas phase. Due to p.b.c. in (b) and (c) the wall terminates the vapor-gas phase in  $z$ -direction. The scale is given by  $l \approx 16\sigma$ .

reference system. Initially liquid and gas particles are located on a lattice ('fluid cube') in the center of a rectangular simulation box, Fig. 1(a). After an equilibration period of  $10^6$  time steps, which consists of a series of subsequent microcanonical simulations at  $T = 300$  K, the system is in a steady state with a liquid film perpendicular to the  $z$ -axis, in coexistence with its vapor-gas phase (vapor is composed of liquid particles). The total number of particles is  $N = 2916$ . Fig. 2 presents density profiles obtained from time averaging during the production runs ( $10^6$  time steps). One can clearly observe an enrichment of gas in the interfacial region, before the gas density falls off towards its value in the bulk liquid. A gas particle close to the interface experiences attractive forces from particles in the liquid film as well as from the vapor-gas phase. Since the density in the liquid film is much larger than in the vapor-gas phase, the resulting force is directed towards the liquid film, which leads to the nonmonotonous density profile. Fig. 2 also shows the absolute decrease of the enrichment with gas concentration. The relative enrichment, however, stays constant as is shown in the inset of Fig. 2(b), where the profiles are scaled by  $N_g$ , displaying universality.

Does gas change the surface tension  $\gamma$ ? Experiments show that gases decrease  $\gamma$  (which has been proposed to be crucial for bubble nucleation), but the reason was stated to be unknown [15]. Applying the standard Kirkwood-Buff [18] formula to calculate  $\gamma$ , a decrease of  $\gamma$  is found as well, when simulations with  $N_g = 0$  and  $N_g > 0$  are compared. We attribute this to a decrease of the cohesive strength of the liquid at the interface due to the gas enrichment. For the above presented system the decrease is about 2%. Additional simulations show that

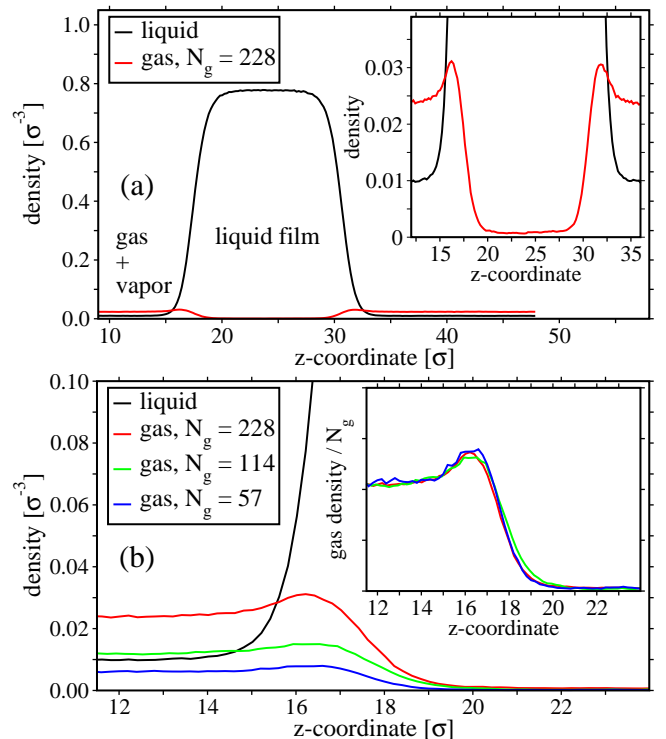


FIG. 2: (color) Density profiles for a liquid-gas mixture in coexistence with its vapor-gas phase. Gas enrichment at the interfaces can be observed in the inset of (a). (b) shows interfacial density profiles for different gas concentrations. The liquid profiles remained essentially unchanged for varying  $N_g$  and only one is displayed in (b). The inset demonstrates that the rescaled gas profiles collapse onto a single curve.

this effect is enhanced for more soluble gases [19] and/or increasing gas pressure, just as in experiments.

What changes in the presence of walls? Since the contact angle  $\theta$  is of vital importance, the walls are first characterized by simulations of droplets, which allows to measure  $\theta$  numerically. A 'fluid cube', composed of only liquid particles ( $N_l = 2916$ ), is initiated on a wall, Fig. 1(b). After equilibration procedures as described above, a droplet (translationally invariant in  $x$ -direction) on a wall in coexistence with its vapor is investigated. Tuning the *microscopic* attraction ratio  $\epsilon_{lw}/\epsilon_{ll}$  (with fixed  $\epsilon_{ll}$ ) results in a change of the *macroscopic* observable  $\theta$ . Using the Laplace estimate of surface energies [18] an estimate  $\theta_L$  for the contact angle is given by [6]  $\cos \theta_L \approx -1 + 2(\rho_w \epsilon_{lw})/(\rho_l \epsilon_{ll})$  with densities  $\rho_w$  and  $\rho_l$  of wall and liquid.  $\rho_l$  is obtained from a simulation of a liquid film as described above. The left part of Fig. 3, (a) to (c), shows density profiles for three different values of  $\epsilon_{lw}/\epsilon_{ll}$  which result in three different contact angles, covering the range from hydrophilic to hydrophobic. Note that apart from the  $\theta \approx 140^\circ$  case  $\theta$  is larger than  $\theta_L$ . This may be related to layering of the liquid (see below) close to the walls, which locally leads to a higher density. According to the expression for  $\theta_L$ , this shifts  $\theta$

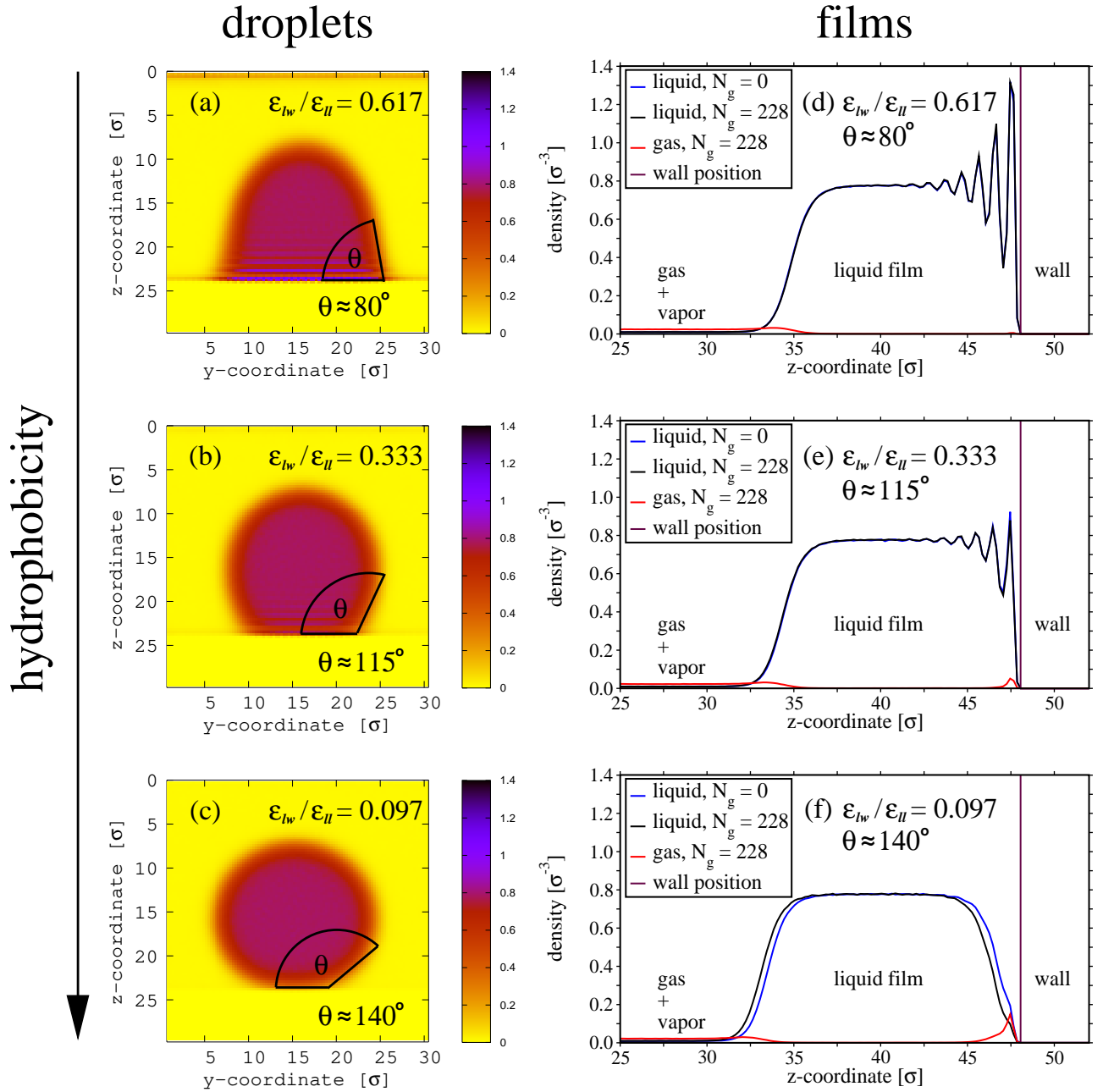


FIG. 3: (color) Left, (a)-(c): Density profiles for droplets at walls, to characterize their hydrophobicity through the contact angle. Right, (d)-(f): Corresponding density profiles for liquid films in contact with a wall and in coexistence with its vapor-gas phase. Note the tremendous increase of the gas density at the hydrophobic walls (e) and (f). (a) and (d): hydrophilic,  $\epsilon_{lw}/\epsilon_{ll} = 0.617 \rightarrow \theta \approx 80^\circ$ ,  $\theta_L \approx 60^\circ$ . (b) and (e): hydrophobic,  $\epsilon_{lw}/\epsilon_{ll} = 0.333 \rightarrow \theta \approx 115^\circ$ ,  $\theta_L \approx 101^\circ$ . (c) and (f): very hydrophobic,  $\epsilon_{lw}/\epsilon_{ll} = 0.097 \rightarrow \theta \approx 140^\circ$ ,  $\theta_L \approx 140^\circ$ .

to higher values. There is no layering for the  $\theta \approx 140^\circ$  case, where  $\theta$  and  $\theta_L$  do agree. We do not address the discrepancy between  $\theta$  and  $\theta_L$  in detail here, since it does not pose problems for the general characterization of the walls. Finally, including gas particles in these simulations hardly modifies the contact angle.

What is the molecular structure of liquids in contact

with walls, in particular in the presence of dissolved gas? With well controled walls in place, we proceed to investigate this issue. Therefore a 'fluid cube' is initiated close to a wall, Fig. 1(c). After equilibration ( $5.25 \times 10^6$  time steps) the system consists of a fluid film in phase coexistence on one side and which is in contact with a wall on the other side. In order to probe the *effect of dissolved gas*

we are going to compare simulations with  $N_g = 0$  (pure liquid) to simulations with  $N_g > 0$  (liquid-gas mixture). Additionally, we investigate the *effect of hydrophobicity* by changing  $\epsilon_{lw}/\epsilon_{ll}$  according to the cases presented in the left part of Fig. 3. The right part of Fig. 3 shows density profiles for  $N_g = 0$  and  $N_g > 0$  and for varying contact angle. The number of liquid and gas particles are  $N_l = 2688$  and  $N_g = 228$ . One immediately observes layering of the liquid [6, 20] which decreases for increasing contact angle and even disappears for the  $\theta \approx 140^\circ$  case, where the liquid density close to the wall is considerably reduced. Introduction of gas in the hydrophilic case, Fig. 3(d), has no important influence on the liquid structure. Nevertheless, even at the hydrophilic wall there is a slight increase of the number of gas particles, which is too small to be observed on the scale adopted in Fig. 3. Increasing the contact angle, adsorption of gas at the wall is drastically increased by a factor  $\approx 50$  for  $\theta \approx 115^\circ$  and more than two orders of magnitude for  $\theta \approx 140^\circ$  when compared to the gas density in the bulk liquid, as is depicted in Fig. 3(e) and (f). Furthermore, the presence of dissolved gas can considerably alter the liquid structure at the wall. In Fig. 3(f) the liquid avoids the wall, placing a 'gas buffer' between liquid and wall, where the density of gas particles is larger than that of liquid particles. The width of the region of gas enrichment is of the order of  $\sigma$ , thus, we basically find a monolayer of gas particles adsorbed at the wall. Energetically it is favorable for gas particles to be subjected to the condensed phases of the liquid and the wall at the interface, while the energetic contribution from liquid-wall interactions, which is diminished by the gas enrichment, is small for hydrophobic walls. Hence, the gas enrichment is supposed to decrease the total energy of the system. However, apart from this qualitative energetic argument we do not have a detailed thermodynamic description of the gas enrichment. We checked (for  $\theta \approx 140^\circ$ ) that gas density profiles with different values of  $N_g$  collapse onto a single curve when rescaled with  $N_g$  (similar to Fig. 2(b)), as expected for low gas concentration and negligible gas-gas interactions.

Our results support the experimental findings that gases dissolved in liquids can have a tremendous influence on the liquid-wall interface. The dramatic increase of gas particles at walls obviously resembles *surface nanobubbles*. Note that the simulated walls were flat, i.e., wall particles were placed on a perfect lattice without wall roughness. For rough walls, one may envision that adsorbed gas accumulates in 'pockets' which one can always find on real surfaces. These gas-pockets would then act as nucleation sites for bubble nucleation. Similarly, the observed 'gas buffer' will decrease the viscosity in the vicinity of walls, which will increase the *slip length* inferred from experiments [1]. We propose that in future studies concerned with nanoscale bubbles and slippage, dissolved gas should be taken into account. Hence, the

presented findings offer important perspectives for further research, which we hope to stimulate by this Letter. Moreover, a detailed study of the dependence of the generic features we have reported on parameters such as solubility, pressure or temperature is important as well.

In conclusion, we have performed molecular dynamics simulations to probe the effects of dissolved gas on liquid-gas and liquid-wall interfaces. At liquid-gas interfaces gas enrichment is found which decreases the surface tension. At liquid-wall interfaces gas enrichment is observed as well, which increases with the contact angle, and can be more than two orders of magnitude for hydrophobic walls, when compared to the gas concentration in the bulk liquid. The presence of gas significantly changes the structure of the liquid close to hydrophobic walls, and will favor bubble nucleation and slippage, just as experimentally observed.

We thank the group of D.E. Wolf for technical support, in particular G. Bartels and L. Brendel. S.M.D. acknowledges financial support (research grant DA969/1-1) from the German Research Foundation (DFG).

---

- [1] E. Lauga, M.P. Brenner, and H.A. Stone, in *Handbook of Experimental Fluid Dynamics*, edited by C. Tropea, J. Foss, and A. Yarin (Springer, New York 2005, in press); C. Neto *et al.*, Rep. Prog. Phys. **68**, 2859 (2005).
- [2] S. Granick, Y. Zhu, and H. Lee, Nature Materials **2**, 221 (2003).
- [3] C. Cottin-Bizonne *et al.*, Phys. Rev. Lett. **94**, 056102 (2005).
- [4] E. Bonaccurso, M. Kappl, and H.J. Butt, Phys. Rev. Lett. **88**, 076103 (2002).
- [5] C. Cottin-Bizonne *et al.*, Eur. Phys. J. E **15**, 427 (2004).
- [6] J.-L. Barrat and L. Bocquet, Phys. Rev. Lett. **82**, 4671 (1999).
- [7] N.V. Priezjev and S.M. Troian, Phys. Rev. Lett. **92**, 018302 (2004).
- [8] P.G. de Gennes, Langmuir **18**, 3413 (2002).
- [9] J.W.G. Tyrrell and P. Attard, Phys. Rev. Lett. **87**, 176104 (2001).
- [10] A.C. Simonsen, P.L. Hansen, B. Klösgen, J. Colloid Interface Sci. **273**, 291 (2004).
- [11] M. Holmberg *et al.*, Langmuir **19**, 10510 (2003).
- [12] M. Switkes and J.W. Ruberti, Appl. Phys. Lett. **84**, 4759 (2004).
- [13] R. Steitz *et al.*, Langmuir **19**, 2409 (2003).
- [14] T. Koishi *et al.*, Phys. Rev. Lett. **93**, 185701 (2004).
- [15] S.D. Lubetkin, Langmuir **19**, 2575 (2003).
- [16] E. Lindahl, B. Hess, and D. van der Spoel, J. Mol. Mod. **7**, 306 (2001).
- [17] H.J.C. Berendsen *et al.*, J. Chem. Phys. **81**, 3684 (1984).
- [18] For a review see J.S. Rowlinson and B. Widom, *Molecular Theory of Capillarity*, (Dover Publications, Mineola, New York 2002, republication).
- [19]  $\epsilon_{gl} = \sqrt{\epsilon_{gg}\epsilon_{ll}} \approx 0.7k_BT$  (Berthelot rule) increases the solubility and the interfacial gas enrichment, and decreases  $\gamma$  by about 10% compared to the  $N_g = 0$  case.

[20] F. Mugele and M. Salmeron, Phys. Rev. Lett. **84**, 5796 (2000).